ACS ORGANIC & INORGANIC Au
AN OPEN ACCESS JOURNAL OF THE AMERICAN CHEMICAL SOCIETY

pubs.acs.org/orginorgau
Article

N-Heterocyclic Carbene-Borane Adducts with Chiral (*R*)-Chloroethyl and Vinyl Substituents

Germán Rodríguez-López, Tayde O. Villaseñor-Granados, Sonia Sánchez-Ruiz, Adriana Esparza-Ruiz,* and Angelina Flores-Parra*

Cite This: *ACS Org. Inorg. Au* 2025, 5, 136−143
Read Online
ACCESS | Metrics & More | Article Recommendations | Supporting Information

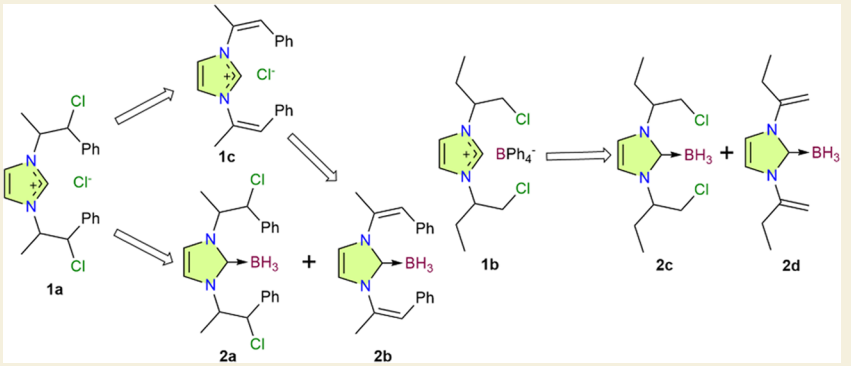

ABSTRACT: This research provides how chiral imidazolium salts {1,3-bis[1′-chloro-1′-phenylpropan-2′-yl]-imidazolium} (**1a**) and enantiopure {1,3-bis[(*R*)-1-chlorobutan-2-yl]-imidazolium} [**1b**] can be utilized in diverse synthetic pathways to obtain new carbene-borane adducts (**2a**−**2d**): {1,3-bis[1′-chloro-1′-phenylpropan-2′-yl]-imidazolyl-2-ylidene-borane} (**2a**), {1,3-bis[(*Z*)-1′-phenylpropen-2′-yl]-imidazolyl-2-ylidene-borane} (**2b**), {1,3-bis[(*R*)-1-chlorobutan-2-yl]-imidazolyl-2-ylidene-borane} (**2c**), and {1,3-bis[but-1-en-2-yl]-imidazolyl-2-ylidene-borane} (**2d**). The carbene-borane adducts were synthesized and characterized by ^{13}C, ^{1}H, and ^{11}B nuclear magnetic resonance spectroscopy and time-of-flight mass spectrometry. The X-ray crystal analyses of compounds **2a** and **2b** were performed, and to understand the structure and interactions of **2a**, a computational study was carried out. The effect of *N*-substituents in the NHC-borane adducts was clearly observed in the C−B bond lengths obtained by single-crystal X-ray diffraction, where the C−B bond is longer for adducts with *N*-(*R*)-chloroethyl substituents than for vinyl substituents. The analysis of the reduced density gradient and the bond critical point calculations of **2a** showed intramolecular proton−hydride and Cl···N interactions. These chiral imidazolium salts could have applicability in the development of new materials and possibly in pharmaceutical research.

KEYWORDS: *N-heterocyclic carbene-borane adducts, dehydrochlorination reaction, intramolecular interactions, X-ray diffraction, electronic structure calculations*

INTRODUCTION

The interest in imidazolium salts and *N*-heterocyclic carbenes (NHCs) arises from their wide applications in organic catalysis,[1] organometallic catalysis,[2] green solvents,[3,4] and therapeutic agents,[5−8] among others.[9−11] Specifically, NHC−BH_3 have potential application as dual reagents for the synthesis and stabilization of metallic nanoparticles such as platinum,[12] palladium, iridium, and gold,[13] due to their easy-to-synthesize nature and the formation of strong and covalent carbon−metal bonds. Also, NHCs can act as strong σ-donors and can coordinate metal ions to form metal NHC complexes, such as platinum, which show anticancer activities.[14] Although boryl radicals were considered elusive species, the relative stability and straightforward synthesis of NHC−BH_3 adducts and NHC−boryl radicals have rapidly expanded their chemistry and synthetic applications.[15,16]

On the other hand, it is well-known that *N*-substituents can modulate the steric effect, chirality induction, and reactivity of NHC−metal complexes and NHC organocatalysts. Particularly, *N*-substituents play a crucial role in the reactivity of NHC−BH_3 adducts, as in the case of 1,3-dimethylimidazole-2-ylidene-borane, which is a more reactive agent for the

Received: December 2, 2024
Revised: January 3, 2025
Accepted: January 7, 2025
Published: January 17, 2025

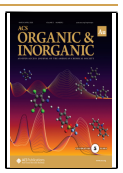

reduction of xanthates (and related functional groups) compared to 1,3-bis(diisopropylphenyl)imidazole-2-ylidene-borane.[17] Unlike conventional bulky aromatic nitrogenous substituents used in NHC−organometallic complexes, *N*-alkyl substituents are regularly used in NHC−boryl radical reactions such as C−C[18] or C−H[19] bond formation, xanthate reduction,[17] and polymerization[20] to name a few.[15,16] We are interested in synthesizing NHC−BH_3 adducts with chiral alkyl substituents derived from the *N*-*β*-chloroethyl imidazolium salts. In this work, we have used the diastereomeric and racemic mixture of {1,3-bis[1′-chloro-1′-phenylpropan-2′-yl]-imidazolium} (**1a**) and enantiopure {1,3-bis[(*R*)-1-chlorobutan-2-yl]-imidazolium} (**1b**, Figure 1).

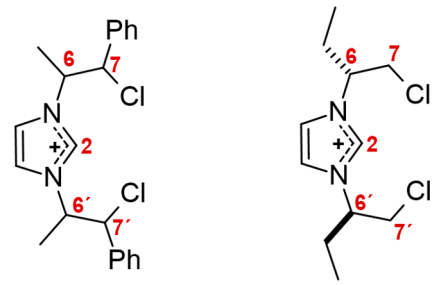

Figure 1. Structure of *N*-(*R*)-chloroethyl imidazolium cations. **1a** was used as a diastereomeric and enantiomeric mixture, and **1b** was used as an enantiopure salt.

Imidazolium salts with (*R*)-chloroethyl substituents can have three different reactive sites: (a) the nucleophilic substitution of chlorine, (b) the elimination reaction or dehydrochlorination, and (c) carbene formation by the deprotonation of the imidazolium ring (Figure 2). Nucleophilic substitutions of *N*-(*R*)-chloroethyl imidazolium or benzimidazolium salts have been reported in the synthesis of PCP complexes by nucleophilic substitution with potassium alkyl phosphides,[21−23] while the elimination reaction of *N*-*β*-chloroethyl imidazolium has only been reported by Cariou.[24] In addition, they also reported the formation of *N*-vinyl substituents via C−H activation of the *N*-(*R*)-chloroethyl group by a Ru(II) complex (Figure 2).[24] In our previous reports on weak nonclassical interactions (Cl···N and C−H···Ag),[25−27] we have described the importance of *N*-(*R*)-chloroethyl substituents in the structure of NHC−Ag complexes. Here, we discuss the reactivity of *N*-substituents **1a** and **1b** in the preparation of four different NHC−BH_3 adducts (**2a**−**2d**). The four carbene-borane adducts were synthesized and characterized by ^{13}C, ^{1}H, and ^{11}B NMR spectroscopy, and TOF-MS spectrometry and X-ray crystal analyses of compounds **2a** and **2b** were performed. To understand the structure and interactions of **2a**, a computational study was carried out.

EXPERIMENTAL SECTION

All of the reagents were used as received without further purification. Standard Schlenk line, glovebox, and vacuum line techniques were employed under an atmosphere of nitrogen. THF was dried by distillation from sodium/benzophenone under an argon atmosphere. CH_2Cl_2 was dried with CaH_2. Deuterated solvents, dry $CDCl_3$, and THF-d_8 were purchased from Sigma-Aldrich. Imidazolium **1a** and **1b** were synthesized, as reported before.[25]

The multinuclear NMR spectra were obtained with different equipment: a Jeol GSX-270 with observation frequencies of 270.16 MHz (^{1}H), 67.93 MHz (^{13}C), and 86.68 MHz (^{11}B). A Jeol Eclipse 400 MHz with observation frequencies of 399.78 (^{1}H), 100.52 (^{13}C), and 128.26 MHz (^{11}B). A Bruker Advance Spectrometer at 300 MHz with observation frequencies of 300.13 MHz (^{1}H), 75.46 MHz (^{13}C), and 96.29 MHz (^{11}B). The assignment of ^{13}C and ^{1}H NMR signals was based on HSQC 2D experiments. The Fourier transform infrared (FTIR) spectra were obtained on the KBr pellet using a PerkinElmer GX spectrometer. The spectra were obtained in the 4000−400 cm^{-1} range. High-resolution mass spectra were obtained by LC/MSD TOF on an Agilent Technologies instruments with ESI as the ionization source.

1,3-Bis[(*Z*)-10-phenylprop-1′-en-2′-yl]-imidazolium Chloride (1c)

A suspension of compound **1a** (0.95 g, 2.3 mmol) and NaHS (0.39 g, 6.9 mmol) in methanol (30 mL) was refluxed for 14 h. Then, the solvent was evaporated in vacuum, and the reaction mixture was suspended in CH_2Cl_2. The solid was filtered and discarded. The solution was evaporated. The solid was washed with acetone (3 × 10 mL). Compound **1c** is a white solid (0.62 g, 80%). It was crystallized by the slow evaporation of a CH_2Cl_2 solution. Mp 240−241 °C. IR, $\nu(cm^{-1})$: 1668 (C═C), 1157 (C═N), 1179 (C——N), 701 (Ph). ^{1}H NMR ($CDCl_3$, 270 MHz): δ 11.01 (s, 1H), 7.19 (m, 6H), 6.95 (s, 2H), 6.89 (m, 4H), 6.59 (s, 2H), 2.51 (s, 6H). $^{13}C\{^{1}H\}$ NMR ($CDCl_3$, 270 MHz): δ 137.9, 132.5, 131.1, 129.0, 128.7, 128.3, 126.9, 122.3, 23.7. (+) TOF calcd for $[C_{21}H_{21}N_2]^+$, m/z (amu): 301.1699; found 301.1702.

1,3-Bis-[(*R*,*R*)-1′-chloro-1′-phenylpropan-2′-yl]-imidazolyl-2-ylidene-borane (2a)

Compound **1a** (0.13 g, 0.31 mmol) was dissolved in nitromethane and dried with calcium hydride for 1 h. The solution was filtered and evaporated under anhydrous conditions. The white solid was dissolved in THF (20 mL) and cooled at −78 °C, and then 0.25 mL of *t*-butyllithium in pentane (1.3 M, 0.32 mmol) was added and stirred. After 30 min, a solution of DMS-BH_3 was added (2.65 M, 0.13 mL). The reaction mixture was evaporated under vacuum. Compound **2a** is a white solid. It crystallized by slow evaporation of $CDCl_3$ in an NMR tube. IR, $\nu(cm^{-1})$: 2929, 2866 (B−H). ^{1}H RMN ($CDCl_3$, 300 MHz): δ 7.3−6.9 (m, 10H), 6.56 (s), 6.42 (s, 2H), 5.42 (br s, 2H), 5.20 (br s, 2H), 1.25 (br s, 6H), 1.15 (br s, 3H). $^{13}C\{^{1}H\}$ NMR ($CDCl_3$, 300 MHz): δ 172.7, 136.8, 136.5, 129.0, 128.6, 128.1, 128.0, 116.9, 64.2, 58.2, 16.7, 16.3. ^{11}B ($CDCl_3$, 300 MHz): −36.6 (q, ^{1}J (^{11}B, ^{1}H) = 81.7 Hz). (+) TOF calcd for $[C_{21}H_{24}N_2BCl_2]^+$ m/z (amu): 385.1404; found: 385.1406.

1,3-Bis-[(*Z*)-1′-phenylpropen-2′-yl]-imidazolyl-2-ylidene-borane (2b)

Compound **1c** (0.11 g, 0.32 mmol) was dissolved in THF (20 mL) and cooled at −78 °C. Then, 0.20 mL of *n*-butyllithium in hexane (1.6 M, 0.32 mmol) was added and stirred. After 30 min, a solution of DMS-BH_3 was added (2.65 M, 0.13 mL). The reaction mixture was evaporated under vacuum. Compound **2b** is a white solid. It was crystallized by the slow evaporation of $CDCl_3$ in an NMR tube. IR, $\nu(cm^{-1})$: 2344, 2300 (B−H). ^{1}H RMN ($CDCl_3$, 400 MHz): δ 7.19−6.93 (m, 10H), 6.57 (s, 2H), 6.50 (s, 2H), 2.34 (s, 6H), 1.30−1.20 (s, 3H). $^{13}C\{^{1}H\}$ NMR ($CDCl_3$, 400 MHz): δ 172.9, 134.1, 134.0, 128.3, 128.2, 127.7, 126.7, 120.1, 23.5. ^{11}B NMR ($CDCl_3$, 400 MHz): −36.4 [q, $^{1}J(^{11}B,^{1}H)$ = 86.91 Hz]. (+) TOF calcd for $[C_{21}H_{20}N_2B]^+$, m/z (amu): 311.1714; found 311.1719.

1,3-Bis-[(*R*)-1-chlorobutan-2-yl]-imidazolyl-2-ylidene-borane (2c)

Compound **1b** (0.18 g, 0.32 mmol) was dissolved in acetonitrile and dried with calcium hydride for 1 h. The solution was filtered and

https://doi.org/10.1021/acsorginorgau.4c00088
ACS Org. Inorg. Au 2025, 5, 136−143

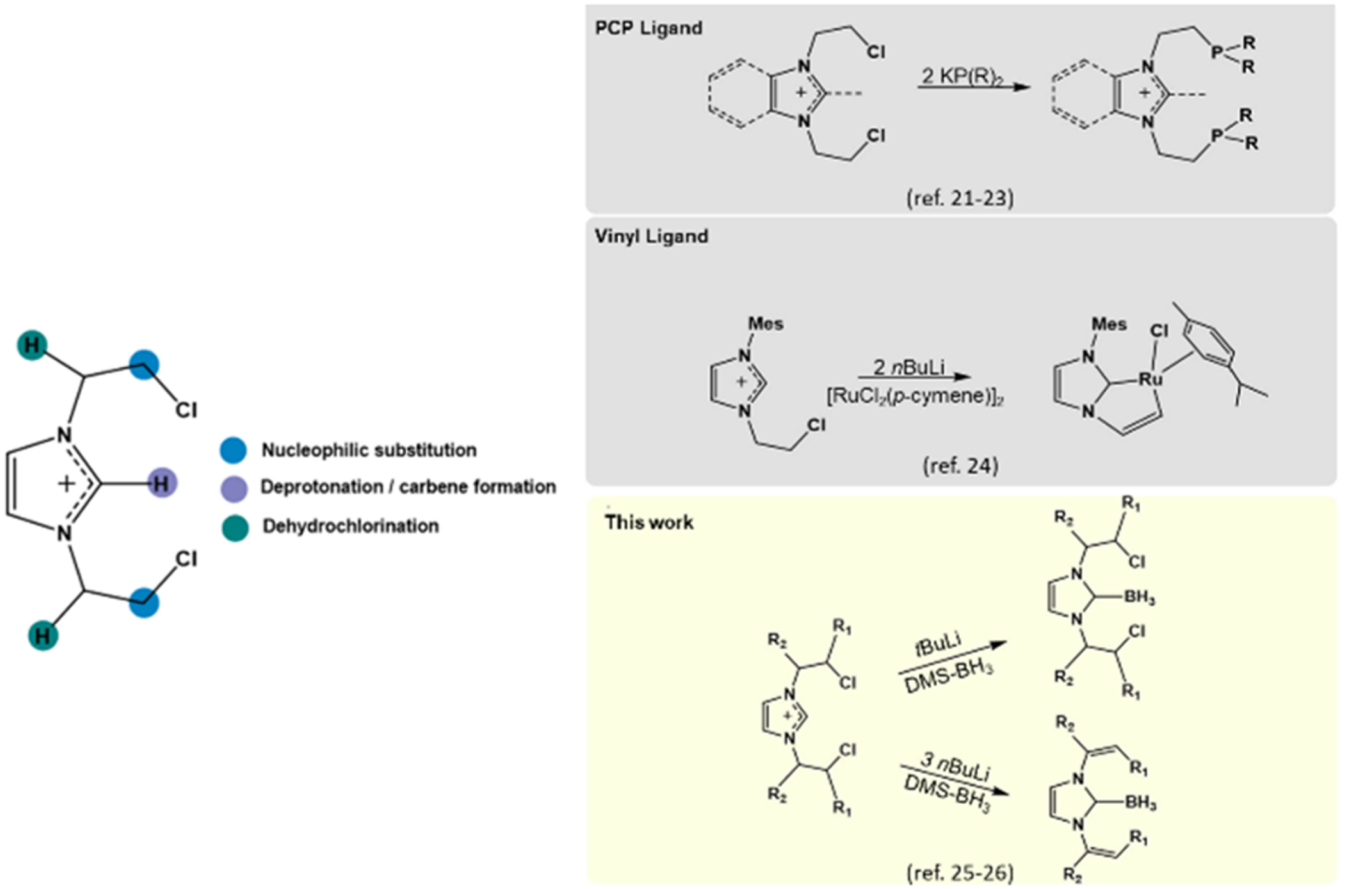

Figure 2. Reactivity and synthesis of different ligands from imidazolium salts with β-chloroethyl substituents.

evaporated in anhydrous conditions. The white solid was dissolved in THF (20 mL) and cooled at −78 °C. Then, 0.25 mL of *t*-butyllithium in pentane (1.3 M, 0.32 mmol) was added and stirred, and after 30 min, a solution of DMS-BH_3 was added (2.65 M, 0.13 mL). The reaction mixture was evaporated under vacuum. Compound **2c** is a white solid. IR, $\nu(cm^{-1})$: 2346, 2284 (B−H). ^{1}H RMN ($CDCl_3$, 300 MHz): δ 6.91 (br s, 2H, H4, H5), 5.10 (br s, 2H, H7), 3.81 (br s, 2H, H6a), 3.76 (br s, 2H, H6b), 1.97 (m, 4H, H8), 1.30−1.20 (s, 3H) 0.91 (t, $^3J(^1H,^1H)$ = 6.7 Hz, 6H, H9). $^{13}C\{^1H\}$ NMR ($CDCl_3$, 300 MHz): δ 167.7 (C2), 117.2 (C4, C5), 59.3 (C7), 46.9 (C6), 24.8 (C8), 10.4 (C9). ^{11}B NMR ($CDCl_3$, 300 MHz): −37.4 (q, $^1J(^{11}B,^1H)$ = 87.2 Hz). (+) TOF calcd for $[C_{11}H_{20}N_2Cl_2B]^+$ *m*/*z* (amu): 261.1091; found: 261.1088.

1,3-Bis[but-1-en-2-yl]-imidazolyl-2-ylidene-borane (2d)

Compound **1b** (0.18 g, 0.32 mmol) was dissolved in acetonitrile and dried with calcium hydride for 1 h. The solution was filtered and evaporated in anhydrous conditions. The white solid was dissolved in THF (20 mL) and cooled at −78 °C; then 0.60 mL of *n*-butyllithium in hexane (1.6 M, 0.96 mmol) was added and stirred, and after 30 min, a solution of DMS-BH_3 was added (2.65 M, 0.13 mL). The reaction mixture was evaporated under vacuum. Compound **2d** is a white solid. IR, $\nu(cm^{-1})$: 2344, 2299 (B−H). ^{1}H NMR ($CDCl_3$, 300 MHz): δ 6.74 (s, 2H), 5.25 (s, 2H), 5.16 (s, 2H), 2.58 (q, ^3J(1H,1H) = 7.3 Hz, 4H), 1.30−1.20 (s, 3H), 1.08 (t, $^3J(^1H,^1H)$ = 7.3 Hz). $^{13}C\{^1H\}$ NMR ($CDCl_3$, 300 MHz): δ 147.8, 120.2, 111.8, 28.1, 11.1. ^{11}B NMR ($CDCl_3$, 300 MHz): − 36.5 (q, $^1J(^{11}B,^1H)$ = 86.2 Hz). (+) TOF calcd for $[C_{11}H_{16}N_2B]^+$, *m*/*z* (amu): 187.1409; found: 187.1401.

Computational Methodology

Conformational analysis was performed in *N*-heterocyclic carbene-borane **2a** to obtain its conformers distribution using the semi-empirical method PM3, which is well-known to predict correct conformations for organic molecules. Then, the minimal energy conformer and performed optimization calculations were chosen using the hybrid method B3LYP functional with the 6 311+ +G(2d,2p) basis set. The same hybrid method was employed to obtain optimized structures and NBO partial charges of the structures using the pseudopotential LANL2DZ with diffuse functions. All these calculations were done using the Gaussian 03 package. Subsequently, Bader analysis of the electronic density was performed with AIMAll software version 17.01.25, which allowed the visualization of bond paths, critical points, and maps of the reduced gradient of the electronic density.

Crystallographic Data

Crystal size, low temperature, long exposure times, and collection strategy were considered to acquire the best possible data set.[25] Crystals **2a** and **2b** were obtained in $CDCl_3$ and measured using a Bruker D8 VENTURE instrument with a PHOTON 100 area detector using graphite monochromatic MoK/a radiation (λ = 0.71073 Å). Even though crystal data were collected up to 0.70 Å resolution, the crystal diffracted quite weakly at high angles, so the data set was cut off for $\sin(\theta)/\lambda > 0.458$ to eliminate noisy, weak data. Crystal structures were solved by direct methods, using SHELXT 2018/2, and refined by full-matrix least-squares methods based on F2 using SHELXL-2019/2. All atoms (except hydrogen atoms) were refined anisotropically. Number CCDC of structures: 2413415 and 1542474 (**2a**) and 2301429 (**2b**) contain the related crystallographic data, which can be obtained free of charge from the Cambridge Crystallographic Data Centre via https://www.ccdc.cam.ac.uk/structures/.

RESULTS AND DISCUSSION

In order to study the reactivity of chiral imidazolium salts *N*-(*R*)-chloroethyl-imidazoliums **1a** and **1b** were prepared as

https://doi.org/10.1021/acsorginorgau.4c00088
ACS Org. Inorg. Au 2025, 5, 136−143

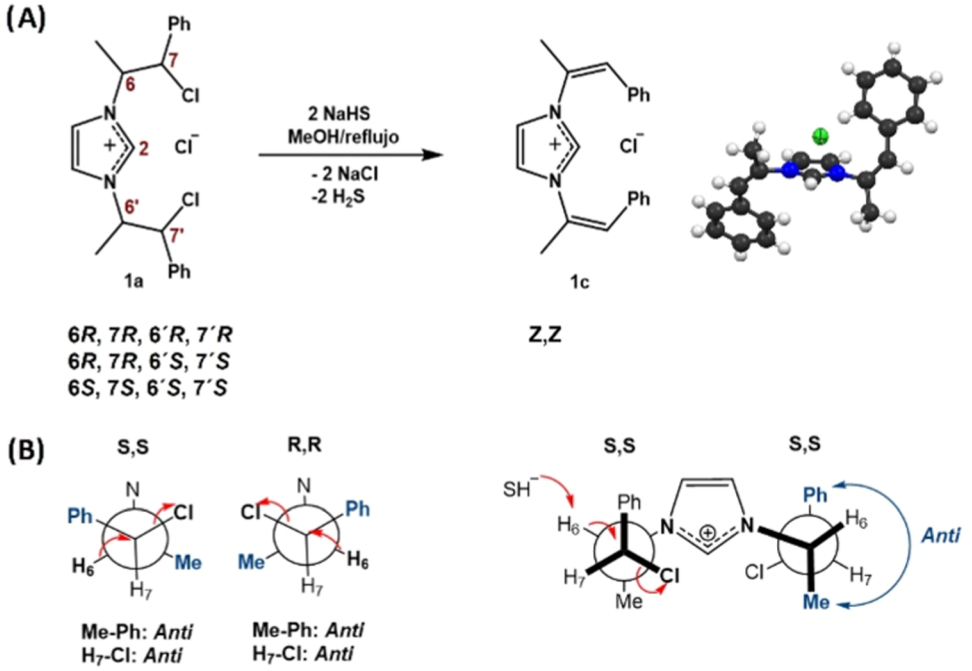

Figure 3. (A) Dehydrochlorination of imidazolium **1a** and the capped stick representation of **1c**. (B) Antiperiplanar arrangement of **1a** for the E2 reaction.

previously reported.[26] The reactivity of the imidazolium was investigated under different reaction conditions, in the presence of (a) lithium diphenylphosphide ($LiPPh_2$) to form PCP ligands, (b) sodium hydrosulfide (NaSH) to form thiols, and (c) *n*BuLi or *t*BuLi as strong bases to give the corresponding carbenes. In the first attempt to form PCP ligands by a nucleophilic substitution reaction between lithium diphenylphosphide and imidazolium **1a**, a mixture of compounds was obtained. The analysis of the ^{31}P NMR spectrum of the reaction mixture showed diphenylphosphine (Ph_2PH, $^{31}P = -40$ ppm), indicating a deprotonation reaction of the imidazolium. Meanwhile, TOF-MS analysis showed dehydrochlorination [M^+-HCl, *m*/*z* (amu): 373.12, 337.14, and 301.17] and degradation of the imidazolium cations.

On the other hand, the reaction of the enantiomeric and diastereomeric mixture of imidazolium **1a** with NaSH produces the complete dehydrochlorination of the *N*-substituents (Figure 3). ^{13}C NMR spectra analysis shows the formation of substituents with only one alkene isomer (C6 and C7, $\delta^{13}C$ = 131.1 and 126.9 ppm, respectively). The diastereomeric selectivity of the reaction allows us to propose an E2 mechanism that produces *Z*-alkenyl substituents (compound **1c**), driven by the antiperiplanar position of the C−H and C−Cl bonds, allowing an antiperiplanar arrangement between the C−Me and C−Ph bonds (Figure 3b). The formation of **1c** was confirmed by single-crystal X-ray diffraction. These results suggest that in contrast to the nucleophilic substitutions reported in the literature for (*R*)-chloroethyl imidazolium,[21−23] the elimination reaction is favored in **1a** and **1b** compounds.

To evaluate the different steric effects, the dehydrochlorination reaction and carbene formation from **1a** and **1b** were studied with different equivalents of strong bases such as *n*-butyllithium (*n*BuLi) and *t*-butyllithium (*t*BuLi), and to obtain the corresponding NHC-BH_3 adducts, DMS−BH_3 was added. The reaction of different *n*BuLi equivalents (1.2, 2.4, or 3) with **1a** gave in high yield a mixture of compound **2a** and traces of **2b** (Figure 4). The reactions of 1.2 equiv of *n*BuLi with **1a**

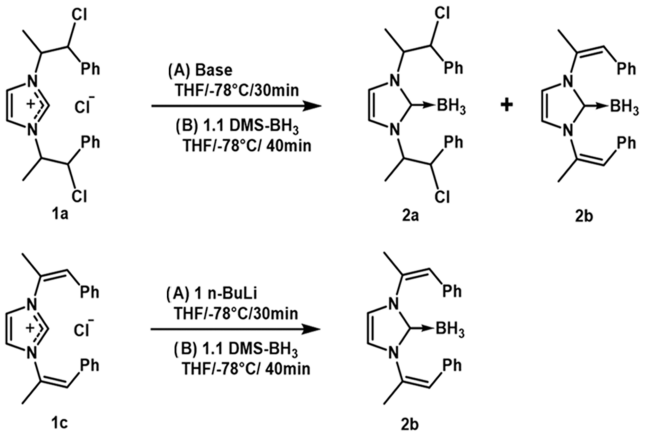

Base	Equivalents	Conv.%	**2a**	**2b**
*n*BuLi	1.2	50	>90 %	traces
*n*BuLi	2.4	>99	>90 %	traces
*n*BuLi	3	>99	>90 %	traces
*t*BuLi	1	>99	100 %	---

Figure 4. Synthesis of NHC-BH_3 adducts **2a** and **2b** in the presence of different base equivalents.

showed regioselectivity deprotonation of C2 with respect to the C6 position, and the presence of *n*BuLi in excess (3 equiv) kept the yield of carbene-borane adduct **2a** above 90%. For the identification of compound **2b**, obtained in traces, it was selectively synthesized from compound **1c**, which was isolated from the mixture reaction of **1a** with NaSH (see above). The reaction to obtain **2b** was carried out in the presence of *n*BuLi and borane.

https://doi.org/10.1021/acsorginorgau.4c00088
ACS Org. Inorg. Au 2025, 5, 136−143

To gain insights into the steric effects of the *N*-substituent, we synthesized imidazolium **1b** with a higher degree of conformational freedom. In contrast to compound **1a**, the reaction of 3 equiv of *n*BuLi with **1b** followed by borane addition produces in quantitatively yields the carbene-borane adducts with vinyl substituents (compound **2d**). On the other hand, the addition of only 1 equiv of *n*BuLi afforded to carbene-borane adducts **2c** and **2d** in a ratio of 2.4:1 (Figure 5). A possible reaction mechanism for compounds **2a**−**2d**,

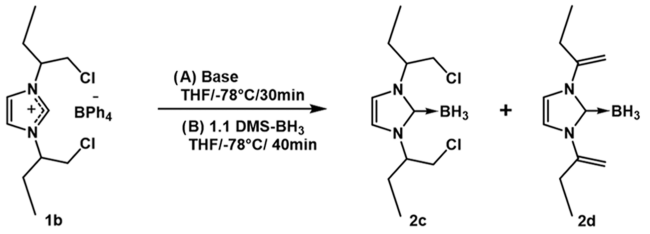

Base	Equivalents	Conv.%	**2c**	**2d**
*n*BuLi	1	64	45 %	19 %
*n*BuLi	3	>90	---	90 %
*t*BuLi	1	80	80 %	---

Figure 5. Synthesis of NHC−BH_3 adducts **2c** and **2d** with different base equivalents.

based on previous reports of a ruthenium(II) compound is proposed.[24] First, without removing the chlorine atom from **1a** or **1b**, the base would abstract the H-2 proton, and then the carbene would bind to BH_3 to form **2a** or **2c**, respectively. In the case of the formation of **2b** or **2d**, there would first be dehydrochlorination and then the abstraction of the H-2 proton from compound **1a** or **1b**, leading to vinyl carbene, followed by coordination to boron. We assume that the conformational freedom of both *N*-substituents and *n*BuLi allows the dehydrochlorination of *N*-substituents and carbene formation. Meanwhile, selective cyclic deprotonation to form **2c** was achieved with *t*BuLi, revealing the strong influence of the steric hindrance of the base.

The obtention of compounds **2c** and **2d** with different equivalents of *n*BuLi or *t*BuLi and the subsequent DMS-borane addition were monitored by ^{11}B NMR, as shown in Figure 6.

The NMR shifts of $^{11}B\{^1H\}$ of **2a**−**2d** (36.6, 36.4, 37.4, and 36.5 ppm) corresponded to adducts of cNH−BH_3, where boron was tetracoordinated with a tetrahedral structure.[15,28] The displacements show a slight tendency of unprotection of boron, **2b** > **2d** > **2a** > **2c**, where unsaturated imidazolium species (**2b** and **2d**) are slightly more unprotected than saturated ones (**2a** and **2c**); they also contain chlorine. It seems that when there is no steric impediment, the chlorines move closer to the boron atom, protecting it slightly, as in **2c**.

In addition, the substituents' effect in the NHC−BH_3 bond was analyzed. Crystals of compounds **2a** and **2b** were suitable for X-ray diffraction (Figures 7 and 8). It is noteworthy that the B−$C_{carbene}$ bond lengths between **2a** {1.609(3)} and **2b** {1.5667(14)} crystal structures are different.

The difference between the two B−$C_{carbene}$ distances is attributed to the *N*-substituents, confirming their importance in the NHC−BH_3 adducts. In Figure 9, the comparison of BH_3−$C_{carbene}$ bond lengths of **2a**, **2b**, and other reported

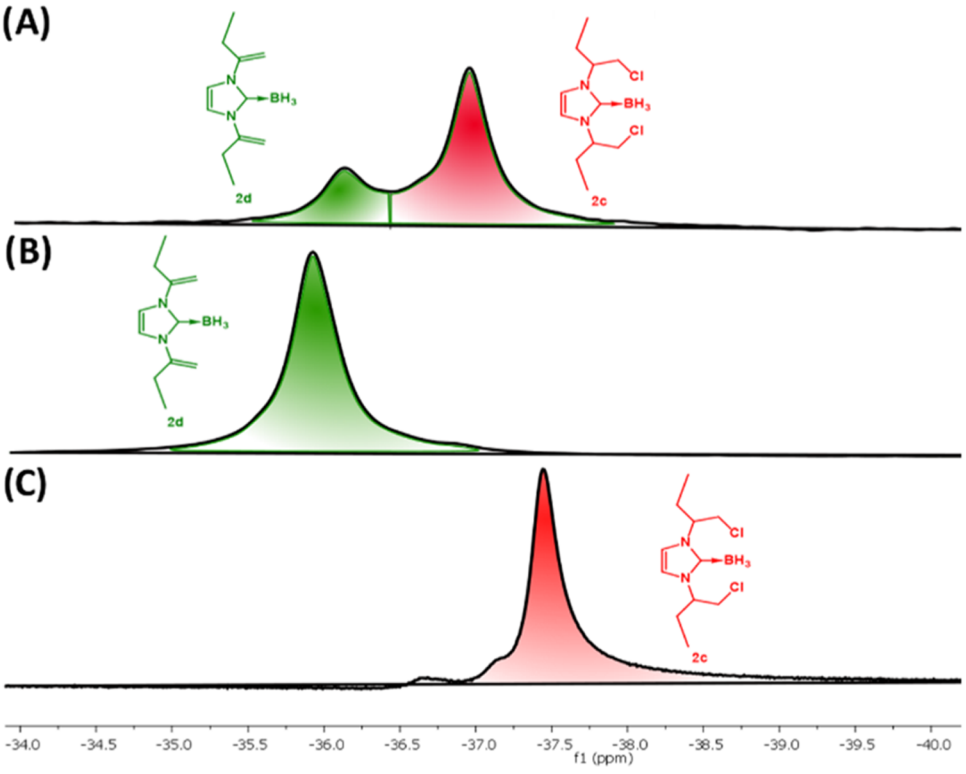

Figure 6. Proton-decoupled $^{11}B\{^1H\}$ NMR spectra (−34.0 to −40.0 ppm) of the reaction products (**2c** and **2d**) obtained of **1b** with different base equivalents: (A) 1 equiv *n*BuLi, (B) 3 equiv *n*BuLi, and (C) 1 equiv *t*BuLi. The green signal corresponds to compound **2d** and the red one to compound **2c**.

https://doi.org/10.1021/acsorginorgau.4c00088
ACS Org. Inorg. Au 2025, 5, 136−143

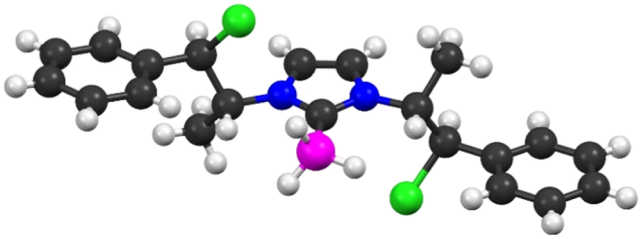

Figure 7. Crystalline structure of **2a**.

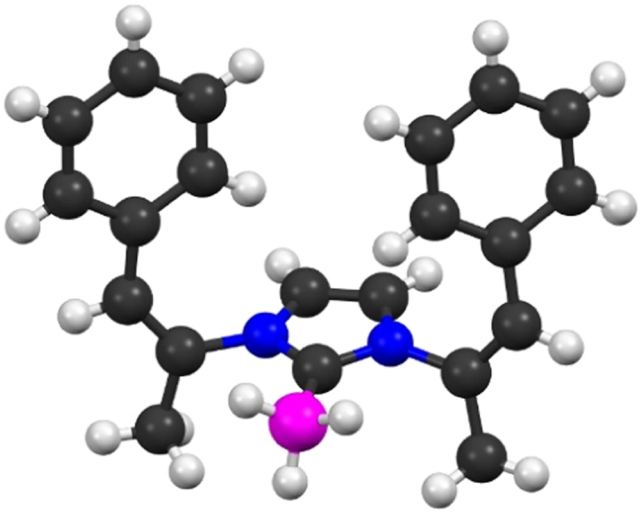

Figure 8. Crystalline structure of **2b**.

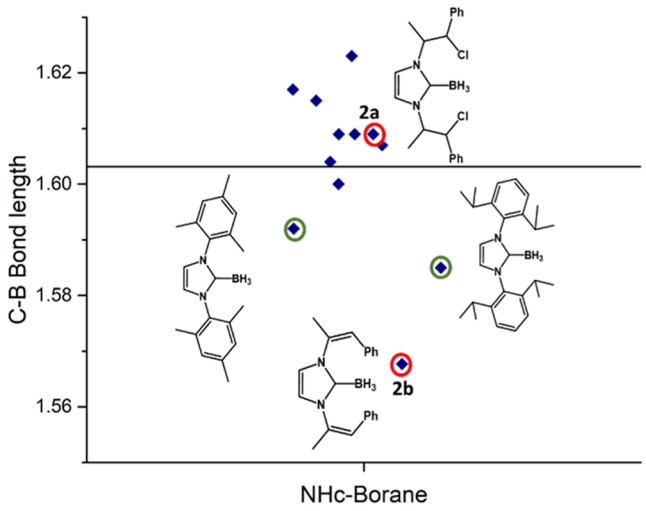

Figure 9. C−B bond lengths of **2a**, **2b**, and *N*-heterocyclic carbene adducts.

structures is shown (see Table S3 in the Supporting Information (SI)).[29−31] Compound **2a** has similar bond distances to other chiral NHC-BH_3 compounds (1.604−1.623 Å),[29] while the bond length of **2b** is even shorter than NHC-BH_3 adducts with aromatic *N*-substituents (1.585−1.596 Å; Figure 10).[30,31]

Furthermore, the crystal structure of **2a** shows that the hydrogens of the *N*-substituents are directed to borane. The distances between the hydrogen of the *N*-substituents and the hydrogens attached to the boron were found to be 2.10, 2.26, and 2.52 Å, smaller than the sum of the van der Waals radii

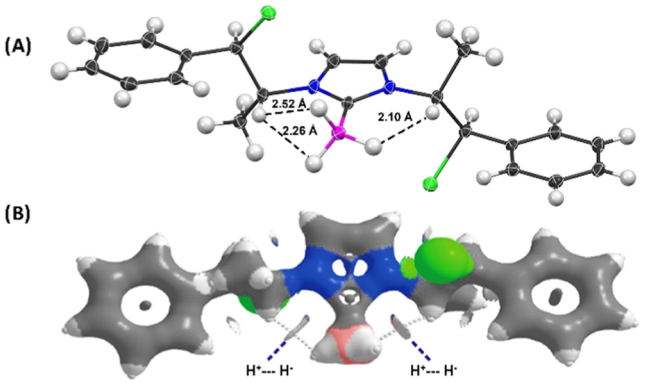

Figure 10. (A) Distances between the α-hydrogen of the *N*-substituents and the borane hydride atom in the crystalline structure of **2a**. (B) Reduced gradient maps and bond critical points of **2a**, showing $H^{\delta+}\cdots H^{\delta-}$ interactions.

[$\sum r_{vdW}(H^{\delta+}\cdots H^{\delta-})$ = 2.65 Å], indicative of hydride−proton interactions (Figure 10A).[32] To better understand the structure and interactions, we performed a computational study using the crystal structure of **2a** as the initial geometry for the calculations. The analysis of the reduced density gradient and the bond critical point calculations show intramolecular proton−hydride interactions (Figure 10B). Cl···N interactions were also observed. These types of interactions have been previously described in *R*-chloroethyl imidazolium and diimines.[25]

The conformation in which the hydrogens of the *N*-substituents are directed toward borane is not only observed in **2a** but also observed in other crystalline structures reported previously. We assume that the inductive effect of nitrogen and the cationic heterocycle increases the hydrogen acidity of the *N*-substituent. The acidity of hydrogen directs the dehydrochlorination of the substituents and even directs the conformation of the adducts in the solid state.

CONCLUSIONS

In summary, we have reported four NHC-borane adducts with alkyl and vinyl substituents. The effect of the *N*-substituents in the NHC-borane adducts is clearly observed in the C−B bond lengths obtained by single-crystal X-ray diffraction, where the C−B bond is longer for adducts with *N*-(*R*)-chloroethyl substituents compared to vinyl substituents. It is noteworthy that the reactivity of the *N*-substituents allowed us to obtain carbene-borane adducts with different structures synthesized from the same imidazolium salt. Our work opens the way to integrating reactive *N*-substituents to diversify structures and properties of *N*-heterocyclic carbene complexes.

ASSOCIATED CONTENT

Data Availability Statement

The data underlying this study are available in the published article and its Supporting Information.

Supporting Information

The Supporting Information is available free of charge at https://pubs.acs.org/doi/10.1021/acsorginorgau.4c00088.

Additional experimental and calculation details; methods and copies of NMR and IR spectra of all products; and crystallographic data of compounds **2a** and **2b** (PDF)

https://doi.org/10.1021/acsorginorgau.4c00088
ACS Org. Inorg. Au 2025, 5, 136−143

Accession Codes

Deposition Numbers 1542474, 2301429, and 2413415 contain the supporting crystallographic data for this paper. These data can be obtained free of charge via the joint Cambridge Crystallographic Data Centre (CCDC) and Fachinformationszentrum Karlsruhe Access Structures service.

AUTHOR INFORMATION

Corresponding Authors

Adriana Esparza-Ruiz − *Faculty of Chemical Engineering, Autonomous University of Yucatan, Mérida, Yucatán 97203, México*; Email: adriana.esparza@correo.uady.mx

Angelina Flores-Parra − *Department of Chemistry, Center for Research and Advanced Studies of the National Polytechnic Institute, Mexico City 07000, México*; orcid.org/0000-0003-0345-0659; Email: aflores@cinvestav.mx

Authors

Germán Rodríguez-López − *Department of Chemistry, Center for Research and Advanced Studies of the National Polytechnic Institute, Mexico City 07000, México*; orcid.org/0000-0002-5952-6715

Tayde O. Villaseñor-Granados − *Department of Chemistry, Center for Research and Advanced Studies of the National Polytechnic Institute, Mexico City 07000, México*

Sonia Sánchez-Ruiz − *Department of Chemistry, Center for Research and Advanced Studies of the National Polytechnic Institute, Mexico City 07000, México*

Complete contact information is available at: https://pubs.acs.org/10.1021/acsorginorgau.4c00088

Author Contributions

The project was conceptualized, supervised, administrated, and analyzed by F.-P. The manuscript was written through contributions of all authors. R.-L.: investigation, formal analysis, and methodology. V.-G.: software and investigation. S.-R.: methodology and NMR spectroscopy. E.-R.: investigation, formal analysis, and X-ray analysis. All authors have given approval to the final version of the manuscript. CRediT: **Germán Rodríguez-López** formal analysis, investigation, methodology; **Tayde O. Villaseñor-Granados** investigation, software; **Sonia Sánchez-Ruiz** methodology; **Adriana Esparza-Ruiz** formal analysis, investigation, software, writing - original draft, writing - review & editing; **Angelina Flores-Parra** conceptualization, formal analysis, project administration, supervision.

Notes

The authors declare no competing financial interest.

ACKNOWLEDGMENTS

The authors acknowledge the CINVESTAV-IPN for the facilities of the supercomputers HPC-cluster Xiuhcoatl and Cluster Abacus-I. Also, thanks to CONAHCYT Mexico financial support and fellowships (T.O.V-G. for his postdoctoral scholarship, and G.R.-L. for his Ph.D. scholarship) and to Marco A. Leyva-Ramirez for refining the X-ray diffraction data of compounds.

REFERENCES

(1) Flanigan, D. M.; Romanov-Michailidis, F.; White, N. A.; Rovis, T. Organocatalytic Reactions Enabled by N-Heterocyclic Carbenes. *Chem. Rev.* **2015**, *115* (17), 9307−9387.

(2) Herrmann, W. A. N-Heterocyclic Carbenes: A New Concept in Organometallic Catalysis. *Angew. Chem., Int. Ed.* **2002**, *41* (8), 1290−1309.

(3) Wasserscheid, P.; Keim, W. Ionic Liquids—New "Solutions" for Transition Metal Catalysis. *Angew. Chem.* **2000**, *39* (21), 3772−3789.

(4) Wang, B.; Qin, L.; Mu, T.; Xue, Z.; Gao, G. Are Ionic Liquids Chemically Stable? *Chem. Rev.* **2017**, *117* (10), 7113−7131.

(5) Egorova, K. S.; Gordeev, E. G.; Ananikov, V. P. Biological Activity of Ionic Liquids and Their Application in Pharmaceutics and Medicine. *Chem. Rev.* **2017**, *117* (10), 7132−7189.

(6) Liu, W.; Gust, R. Metal N-Heterocyclic Carbene Complexes as Potential Antitumor Metallodrugs. *Chem. Soc. Rev.* **2013**, *42* (2), 755−773.

(7) Hussaini, S. Y.; Haque, R. A.; Li, J.; Zhan, S.; Tan, K. W.; Razali, M. R. Coinage Metal Complexes of N-heterocyclic Carbene Bearing Nitrile Functionalization: Synthesis and Photophysical Properties. *Appl. Organomet. Chem.* **2019**, *33* (6), No. e4927.

(8) Hindi, K. M.; Panzner, M. J.; Tessier, C. A.; Cannon, C. L.; Youngs, W. J. The Medicinal Applications of Imidazolium Carbene−Metal Complexes. *Chem. Rev.* **2009**, *109* (8), 3859−3884.

(9) Bellotti, P.; Koy, M.; Hopkinson, M. N.; Glorius, F. Recent Advances in the Chemistry and Applications of N-Heterocyclic Carbenes. *Nat. Rev. Chem.* **2021**, *5* (10), 711−725.

(10) Peris, E. Smart N-Heterocyclic Carbene Ligands in Catalysis. *Chem. Rev.* **2018**, *118* (19), 9988−10031.

(11) Smith, C. A.; Narouz, M. R.; Lummis, P. A.; Singh, I.; Nazemi, A.; Li, C.-H.; Crudden, C. M. *N* -Heterocyclic Carbenes in Materials Chemistry. *Chem. Rev.* **2019**, *119* (8), 4986−5056.

(12) Lara, P.; Suárez, A.; Collière, V.; Philippot, K.; Chaudret, B. Platinum N-Heterocyclic Carbene Nanoparticles as New and Effective Catalysts for the Selective Hydrogenation of Nitroaromatics. *ChemCatChem* **2014**, *6* (1), 87−90.

(13) Hippolyte, L.; Sadek, O.; Ba Sowid, S.; Porcheron, A.; Bridonneau, N.; Blanchard, S.; Desage-El Murr, M.; Gatineau, D.; Gimbert, Y.; Mercier, D.; Marcus, P.; Chauvier, C.; Chanéac, C.; Ribot, F.; Fensterbank, L. *N* -Heterocyclic Carbene Boranes: Dual Reagents for the Synthesis of Gold Nanoparticles. *Chem. - Eur. J.* **2023**, *29* (46), No. e202301610.

(14) Zhao, S.; Yang, Z.; Jiang, G.; Huang, S.; Bian, M.; Lu, Y.; Liu, W. An Overview of Anticancer Platinum N-Heterocyclic Carbene Complexes. *Coord. Chem. Rev.* **2021**, *449*, No. 214217.

(15) Curran, D. P.; Solovyev, A.; Makhlouf Brahmi, M.; Fensterbank, L.; Malacria, M.; Lacôte, E. Synthesis and Reactions of N-Heterocyclic Carbene Boranes. *Angew. Chem., Int. Ed.* **2011**, *50* (44), 10294−10317.

(16) Taniguchi, T. Advances in Chemistry of N-Heterocyclic Carbene Boryl Radicals. *Chem. Soc. Rev.* **2021**, *50* (16), 8995−9021.

(17) Ueng, S.-H.; Fensterbank, L.; Lacôte, E.; Malacria, M.; Curran, D. P. Radical Reductions of Alkyl Halides Bearing Electron Withdrawing Groups with N-Heterocyclic Carbene Boranes. *Org. Biomol Chem.* **2011**, *9* (9), 3415−3420.

(18) Wan, T.; Capaldo, L.; Ravelli, D.; Vitullo, W.; de Zwart, F. J.; de Bruin, B.; Noël, T. Photoinduced Halogen-Atom Transfer by *N* -Heterocyclic Carbene-Ligated Boryl Radicals for C(Sp^3)−C(Sp^3) Bond Formation. *J. Am. Chem. Soc.* **2023**, *145* (2), 991−999.

(19) Pan, X.; Lacôte, E.; Lalevée, J.; Curran, D. P. Polarity Reversal Catalysis in Radical Reductions of Halides by N-Heterocyclic Carbene Boranes. *J. Am. Chem. Soc.* **2012**, *134* (12), 5669−5674.

(20) Tehfe, M.-A.; Monot, J.; Brahmi, M. M.; Bonin-Dubarle, H.; Curran, D. P.; Malacria, M.; Fensterbank, L.; Lacôte, E.; Lalevée, J.; Fouassier, J.-P. N-Heterocyclic Carbene-Borane Radicals as Efficient Initiating Species of Photopolymerization Reactions under Air. *Polym. Chem.* **2011**, *2* (3), 625−631.

(21) Iglesias, M.; Iturmendi, A.; Sanz Miguel, P. J.; Polo, V.; Pérez-Torrente, J. J.; Oro, L. A. Tuning PCP−Ir Complexes: The Impact of

an N-Heterocyclic Olefin. *Chem. Commun.* **2015**, *51* (62), 12431−12434.
(22) Lee, H. M.; Zeng, J. Y.; Hu, C.-H.; Lee, M.-T. A New Tridentate Pincer Phosphine/ *N* -Heterocyclic Carbene Ligand: Palladium Complexes, Their Structures, and Catalytic Activities. *Inorg. Chem.* **2004**, *43* (21), 6822−6829.
(23) Huynh, H. V.; Meier, N.; Pape, T.; Hahn, F. E. Benzothiazolin-2-Ylidene Complexes of Iridium(I). *Organometallics* **2006**, *25* (12), 3012−3018.
(24) Cariou, R.; Fischmeister, C.; Toupet, L.; Dixneuf, P. H. A Bidentate NHC−Alkenyl Ruthenium(II) Complex via Vinyl C−H Bond Activation. *Organometallics* **2006**, *25* (9), 2126−2128.
(25) Rodríguez-López, G.; Montes-Tolentino, P.; Sánchez-Ruiz, S.; Villaseñor-Granados, T. O.; Flores-Parra, A. Cl···N Weak Interactions. Conformational Analysis of Imidazol-2-Ylum Heterocycles Bearing N -*β*-Chloroethyl and N -Vinyl Pendant Groups. *J. Mol. Struct.* **2017**, *1148*, 213−222.
(26) Rodríguez-López, G.; Montes-Tolentino, P.; Villaseñor-Granados, T. O.; Flores-Parra, A. New Silver Imidazol-2-Ylidene Complexes with Pendant N-*β*-Chloroethyl and N-Vinyl Groups. Cl···N and C-H···Ag Weak Interactions. *J. Organomet. Chem.* **2017**, *848*, 166−174.
(27) Villaseñor-Granados, T. O.; Rodríguez-López, G.; Ramos-García, I.; Morales-Martínez, D.; González, F. J.; Flores-Parra, A. Linkage between Fluorescence and Electrochemical Properties of Imidazolium Compounds in Acetonitrile Solution. *ChemPhysChem* **2020**, *21* (11), 1177−1183.
(28) Solovyev, A.; Lacôte, E.; Curran, D. P. Ring Lithiation and Functionalization of Imidazol-2-Ylidene-Boranes. *Org. Lett.* **2011**, *13* (22), 6042−6045.
(29) Banerjee, D.; Besnard, C.; Kündig, E. P. Chiral N-Heterocyclic Carbene Borane Complexes: Synthesis and Structural Analysis. *Organometallics* **2012**, *31* (2), 709−715.
(30) Ramnial, T.; Jong, H.; McKenzie, I. D.; Jennings, M.; Clyburne, J. A. C. An Imidazol-2-Ylidene Borane Complex Exhibiting Inter-Molecular [C−H $^{\delta+}$ ···H $^{\delta-}$ − B] Dihydrogen Bonds. *Chem. Commun.* **2003**, No. No. 14, 1722−1723.
(31) Wang, Y.; Quillian, B.; Wei, P.; Wannere, C. S.; Xie, Y.; King, R. B.; Schaefer, H. F.; Schleyer, P. v. R.; Robinson, G. H. A Stable Neutral Diborene Containing a BB Double Bond. *J. Am. Chem. Soc.* **2007**, *129* (41), 12412−12413.
(32) Güizado-Rodríguez, M.; Ariza-Castolo, A.; Merino, G.; Vela, A.; Noth, H.; Bakhmutov, V. I.; Contreras, R. Weak Intramolecular Proton−Hydride and Proton−Fluoride Interactions: Experimental (NMR, X-Ray) and DFT Studies of the Bis(NBH $_3$) and Bis(NBF $_3$) Adducts of 1,3-Dimethyl-1,3-Diazolidine. *J. Am. Chem. Soc.* **2001**, *123* (37), 9144−9152.

https://doi.org/10.1021/acsorginorgau.4c00088
ACS Org. Inorg. Au 2025, 5, 136−143